Final Report

"Continuous Airborne Measurements and Analysis of Oil & Natural Gas Emissions During the 2021 Denver-Julesburg Basin Studies"

Prepared by:

The **A**dvance **L**aser **T**echnology for **A**tmospher**i**c **R**esearch (ALTAiR) Laboratory
Institute of Arctic & Alpine Research, the University of Colorado Boulder[1]

&

The Department of Atmospheric & Oceanic Sciences, the University of Maryland[2]

To

Colorado Oil & Gas Conservation Commission (COGCC)

&

The Colorado Air Pollution Control Division, Department of Public Health & Environment (CDPHE)

Report Authors: Drs. Alan Fried[1], Russell Dickerson[2]

Report Contributors: Hannah Daley[2], Hao He[2], Phillip Stratton[2], Dr. Petter Weibring[1], Dr. Dirk Richter[1], James Walega[1]

Dr. Abigail Koss and Dr. Joel Kimmel, TOFWERK USA, Boulder, CO

Dr. Xinrong Ren, NOAA Air Resources Laboratory, Maryland

Dr. Alan Brewer, NOAA, Chemical Sciences Laboratory, Boulder, CO

Dr. Sunil Baidar, NOAA, Chemical Sciences Laboratory, Boulder, CO & CIRES, University of Colorado, Boulder, CO

Period of Performance: May 1, 2021 – April 30, 2023

Date of this Report: May 9, 2023

1.0 Executive Summary of Final Results

This report summarizes measurements and analyses for fall 2021 flights over the Denver-Julesburg Basin (DJB) to determine emissions from oil and natural gas (O&NG) operations. It is a follow up to our interim report submitted on July 5, 2022. The interim report presented mass balance top-down emission fluxes over the DJB for methane (CH_4) and ethane (C_2H_6) resulting from a suite of airborne measurements acquired on October 1 and October 5, 2021. Since the interim report, we carried out a more detailed updated analysis effort on these two flight days to further support our mass balance results and error analysis as well as provide more rigorous estimates for the percentage of methane over the DJB associated with O&NG drilling operations and from Concentrated Animal Feeding Operations (CAFOs). Sections 3 - 6 of this report summarize the mass balance calculations and updated final analysis efforts, highlighted in boldface. Table 1 presents the interim values for emission rates (ER) provided in the July 5, 2022 report from the University of Colorado (CU) and University of Maryland (UMD) teams. Table 2 presents the final ER results based upon our reanalysis efforts, which reveal small changes to our interim values. These final results will be submitted to an appropriate journal in the near future for refereed publication(s). This final report represents fulfillment of the contractual obligations of CU and UMD to CDPHE and COGCC.

Table 1: Results Presented in the July 5, 2022 Interim Report

Study Period	Total CH_4 ER 10^6 g/hr	O&NG CH_4 ER Estimates 10^6 g/hr	Total C_2H_6 ER 10^6 g/hr
CU/UMD Oct 1, 2021	**19.7 ± 4.2***	**14.4** (73%)**	**1.9 ± 0.6***
CU/UMD Oct 5, 2021	**26.9 ± 7.9***	**22.3** (83%)**	**2.2 ± 0.8***
Averaged CU/UMD	**23.3 ± 4.5**	**18.4 (79%)**	**2.1 ± 0.5**

*The total uncertainty calculated from an error propagation analysis.
**Estimates from the correlation coefficients in the present study

Table 2: Final Results Based Upon Our Reanalysis in This Report & Comparisons with Other DJB Studies. The Emission Rates are in Units of 10^6 g/hr (MT/hr)

Study Period	Total CH_4 ER	O&NG CH_4 % Estimates	Total C_2H_6 ER
Petron May 2012	26.0 ± 6.8	74 ± 33%	
Peischl April 2015	24 ± 5	75% ± 37%	7.0 ± 1.1
Kille March 2015		63% ± 17%	
Univ. of Arizona Sept/Oct 2021	25 ± 7	79%	
This Study Oct. 2021	**25.3 ± 8.4***	**71% ± 10%****	**3.1 ± 1.4***

*The total (systematic + random) uncertainty (1σ level) calculated from an error propagation analysis.
**The average value from two approaches carried out for the Oct. 1 and Oct. 5 flights.

2.0 Overview of Instruments Employed in This Study

The interim report presented an overview of the measurements employed in this study. For completeness, we again present these measurements in this final report. Airborne measurements of various trace gases were acquired employing the Maryland University Research Foundation's (URFs) Cessna 402B research aircraft. The aircraft payload consisted of instruments for continuous 1-second measurements of: 1) ethane (1 Hz) from the CU team employing their

CAMS-2 (Compact Airborne Multispecies Spectrometer-2, Weibring et al., 2020); 2) carbon dioxide, methane, and CO (0.3 Hz) employing the UMD Picarro analyzer; 3) nitrogen dioxide (NO_2) employing the UMD Teledyne Cavity Attenuated Phase Shift analyzer (0.1 Hz); 4) meteorological parameters of air temperature, pressure, relative humidity, wind speed and wind direction employing the UMD Vaisala instrument and differential GPS (1 Hz); and 5) TOFWERK's Vocus Elf Proton Transfer Reaction Time of Flight Mass Spectrometer (PTR-TOF-MS) (1 Hz) measurements of benzene, toluene, xylene, acetone, acetonitrile, acetaldehyde, acetic acid and other volatile organic compounds (VOCs). A total of nine flights were successfully carried from September 17, 2021 – October 5, 2021 over the DJB, and six of which were considered appropriate for mass balance analysis in deriving the flux for methane (CH_4), and ethane (C_2H_6). By agreement with the Colorado Department of Public Health and the Environment (CDPHE), this report summarizes the final results for two of the research flights: Oct. 1, 2021 and Oct. 5, 2021. Additional analysis for the remaining flights, as appropriate, will be carried out in a separately funded effort. Analysis for the two flight days in this report was significantly aided by NOAA Mobile Lidar system. Figure 1 provides photographs of the UMD 402B Cessna Research Aircraft along with the various instruments employed. The UMD instruments are part of the normal aircraft instrument package employed on this aircraft for east coast ozone studies. The CAMS-2 instrument, which successfully acquired ethane measurements on the NASA King Air aircraft, was repackaged to reduce size, weight, and power, specifically for these studies on the smaller Cessna aircraft platform. The TOFWERK's Vocus Elf Proton Transfer Reaction Time of Flight Mass Spectrometer (PTR-TOF-MS), mounted behind the UMD instruments, was also modified to fly on this aircraft platform.

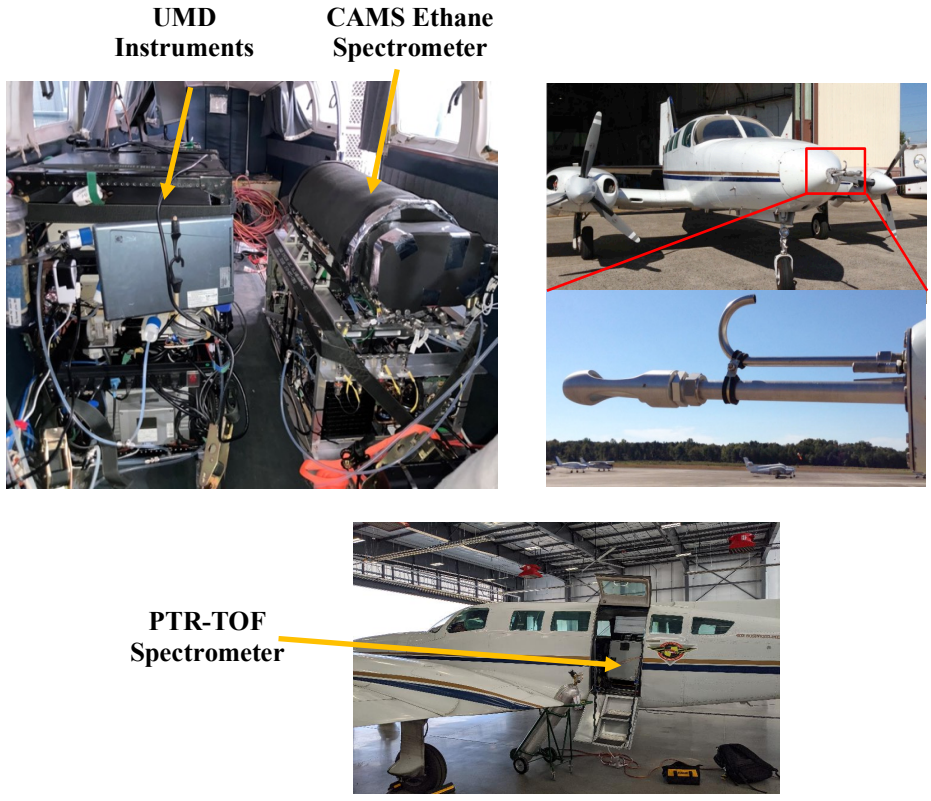

Figure 1: (Top left) Interior of the airplane viewed from the pilot's seat. The CAMS-2 ethane instrument located on the right side next to the door and the various UMD instruments, extending from behind the co-pilot seat to the middle

of the airplane, are located on the left side. The PTR-TOF-MS spectrometer, which is hidden in this view behind the UMD instruments, can be seen in the bottom photograph just inside the aircraft door. The **(right figures)** show the 402B aircraft and the reverse-facing *"candy-cane"* gas inlet in the nose of the aircraft.

Figure 2: Photograph of NOAA's Mobile Lidar Van, which provided spatial, temporal, and vertically resolved wind speed and wind direction measurements along the aircraft inflow and outflow flight legs.

3.0 Overview of the Denver-Julesburg Basin (DJB)

Figure 3 provides an overview of the DJB basin covered by the airborne measurements of this study along with airborne measurements from other studies.

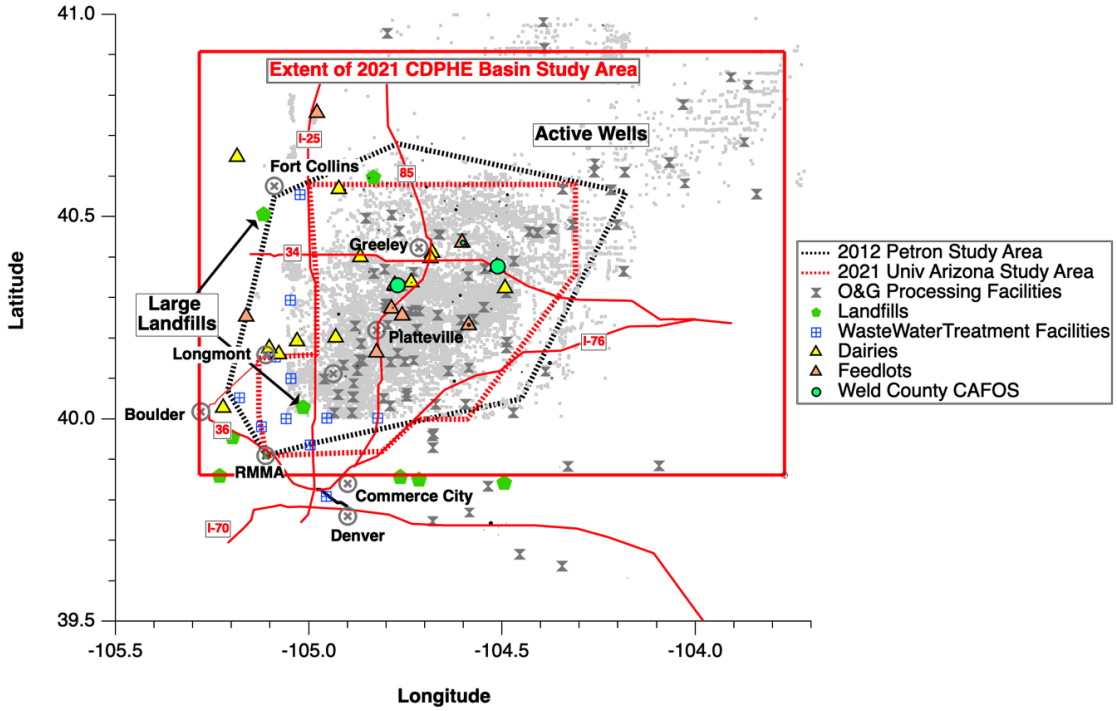

Figure 3: Airborne measurement regime from this study (red rectangle), the 2012 Petron study area, and the 2021 University of Arizona study. The 2015 Peischl study (not shown) covered a very similar region as the Petron study.

The study area for our 2021 airborne measurements extends over the same region as other studies with only a slightly larger area of coverage. These studies include the 2012 study (Pétron et al., 2014), the 2015 Peischl et al. (2018), and the 2021 University of Arizona airborne column measurements by Cusworth et al. (2022) carried out over the same time frame as this study.

The active wells in Weld and Larimer Counties, which by the end of October 2021 numbered over 18,000, are highlighted by the light gray dots. The additional CH_4 sources, denoted by the inset key, are also indicated on this map along with the flight track outlines from the 2012 Pétron and the 2021 University of Arizona studies. This figure shows the extensive nature for the various DJB CH_4 sources, which includes oil and natural gas processing facilities (O&NG), landfills, wastewater treatment facilities, dairies, the largest feedlots and the associated CAFOs facilities (sized by the total animal units). The airplane base of operations for the present study was located at the Rocky Mountain Metropolitan Airport (RMMA). As can be seen, the largest feedlots, dairy, and CAFOs facilities are in close proximity to O&NG facilities and well operations concentrated in the Greeley/Platteville region. Since the various DJB studies span the same emission source regions with only minor geographic differences, the comparative results are meaningful, and this will be discussed in a later section.

Figures 4a,b show the Oct. 1, 2021 flight track colored and sized by the measured airborne CH_4 concentrations (Fig. 4a) and the measured C_2H_6 (Fig. 4b). The CH_4 in Fig. 4a is restricted to 2300 ppb to maintain resolution even though the 1-second values over the two highlighted landfills are 2892 and 2763, respectively, over Erie and the Larimer County landfills. The C_2H_6 values are shown without restriction. Since C_2H_6 is not emitted from landfills, these two maps highlight the value of carrying out simultaneous measurements of both constituents on the same airborne platform.

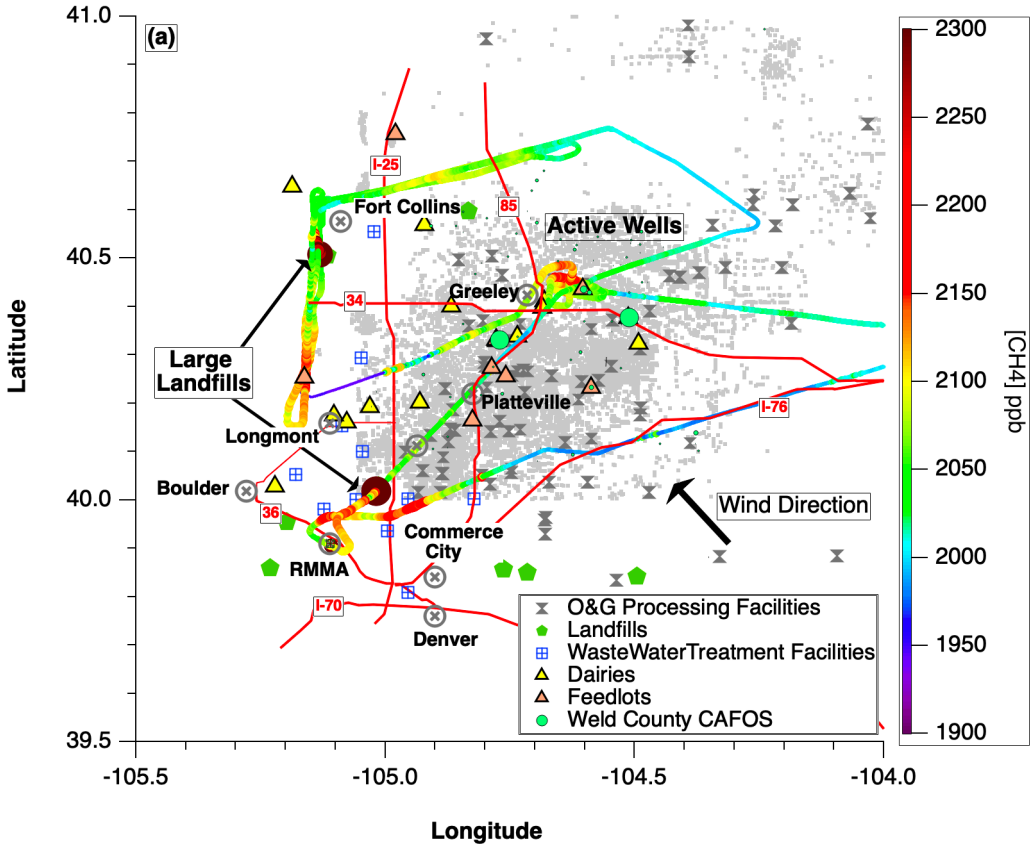

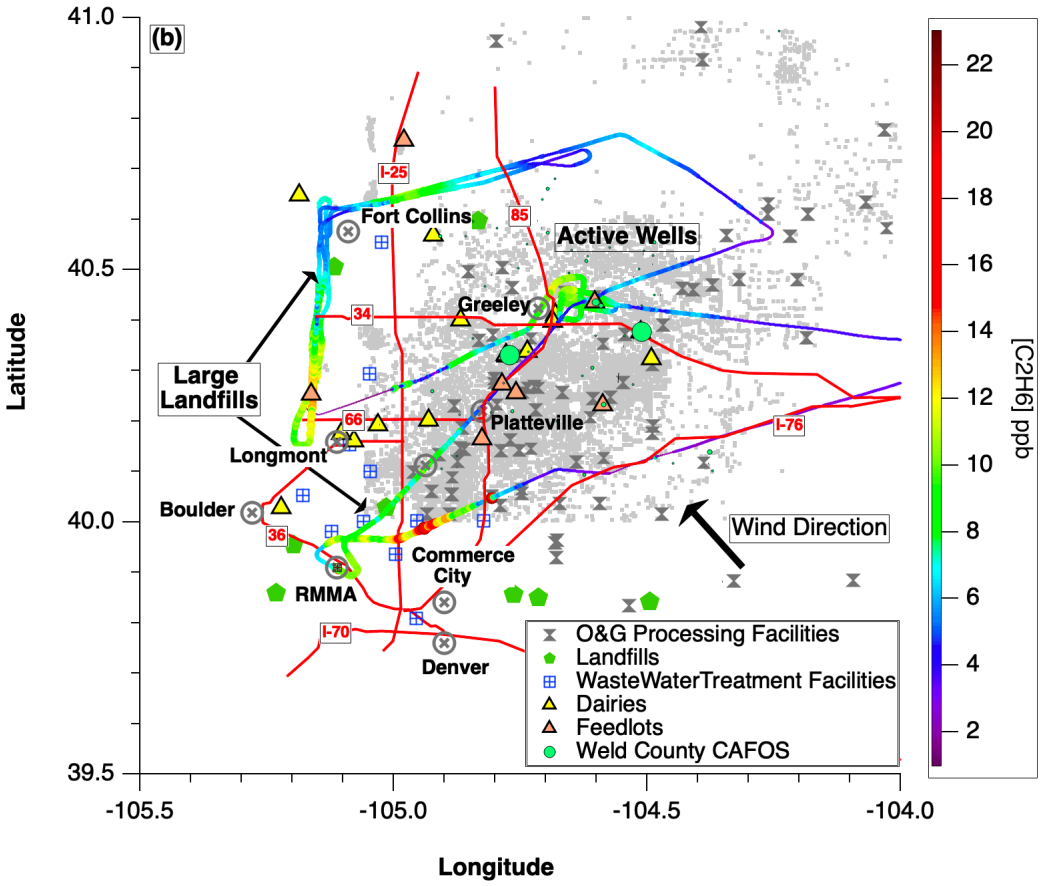

Figures 4 Oct. 1, 2021 flight track with the prevailing wind direction depicted by the large black arrow.

The data on October 1 show the large landfill CH_4 sources, and this is accentuated by the low wind speeds of 2 – 3 m/s. These plots also reveal the importance of properly identifying the active basin influence footprint involved in the mass balance flux determinations. The challenge is to identify upstream inflow *IF* legs, which when traversing the basin uniformly mix in the various emission constituents from the surface to the top of the planetary boundary layer (PBL) due to steady winds. The resulting emission-influenced air masses are then uniquely sampled at various altitudes downwind (outflow *OF* legs), which are only influenced by this flow regime. It is thus essential to identify whether or not highly localized emission sources, such as the two large landfills shown in Fig. 4a, are included in this influence footprint. To accomplish this, we heavily relied on forward and back trajectories employing NOAA's HYSPLIT forward and back trajectory models using the HRRR (High Resolution Rapid Refresh) model, which in turn employs 3 km meteorology. **Our updated analysis included additional HYSPLIT trajectories carried out over finer time steps to better match the aircraft locations and over longer time periods to better extend over the *IF* and *OF* aircraft legs. This analysis was aided by comparing *OF* ethane/methane linear regressions with regressions for the entire basin. This additional step was found to be extremely important in supporting our *OF* leg selections, which best represented the airmass flow over the entire basin. This analysis both removed and added additional *OF* legs not included in our interim report.** As can be seen in the figures above, this analysis guarded against including *OF* legs influenced by large upstream contributions from Commerce City (Suncor Refinery)/Denver VOC sources that were outside of the study area and not represented by the *IF* legs.

4. Mass Balance Emission Flux Determinations for CH_4 and C_2H_6 over the DJB

Figure 5 provides a pictorial representation of the mass balance approach employed in our emission rate (ER) determinations. The emission rates in grams/sec, are converted to our final values in metric tonnes/hour (10^6 grams/hour) by multiplication of the results by 3.60 x 10^{-3}. In this expression, the various terms are as follows: MLH (mixed layer height from z_0 to z_1 in units of m, also referred to as planetary boundary layer depth, PBL); ΔC (concentration difference between the plume outflow *OF* region (X_{Plume}) and the inflow *IF* region (X_{BKG}) in units of ppb), and this difference is multiplied by 10^{-9} to convert ppb to absolute mixing ratios and further multiplied by the molecular weight of the species under study to convert to grams; WS (wind speed in m/s); cos ($WD_{\perp}$ - Heading), the cosine of the angle between the normal to the wind direction (WD) and the aircraft heading (Heading); the aircraft ground speed (GS in m/s); the duration of the plume (ΔT in s); the air number density (N(P,T)) in units of moles m^{-3}. The integration is calculated over the plume width (*dy* from -y to +y in m) and over the MLH (*dz* from the surface z_0 to the top of the boundary layer z_1). To improve measurement precision, all concentration and wind measurements are smoothed using an 11-point box car smooth and these values are employed in the following expression. **The results from this expression were independently compared employing two different source codes: one from the University of Maryland using the MATLAB program and one from the University of Colorado employing the Igor program. The results agreed to within a few tenths of a percent.**

$$ER = \int_{z_0}^{z_1} MLH \} \int_{-y}^{y} (\Delta C)^* (WS)^* \cos (WD_{\perp} - Heading)\ ^*(GS^*\Delta T)^*\{N(P,T)\}\ dz\ dy$$

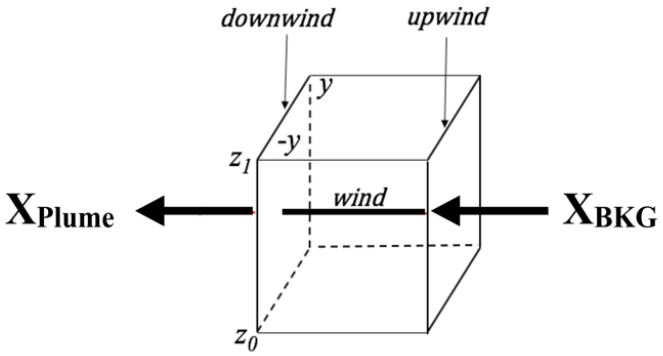

Figure 5: Pictorial representation of the mass balance approach.

The emission rates were determined using the above equation at each of the *OF* sampling altitudes. **Two corrections to these emission rates, which were not included in our interim results, have been applied in this re-analysis. The first is a minor correction (in the ~ ± 5% range) to the airmass density N at the *OF* altitude. This corrects the airmass density at the measurement altitude to the average basin altitude between the surface and the top of the PBL. The second correction utilizes the Mobile Lidar (ML) measurements of wind speed and**

direction. This provides a better representation of the winds from the surface to the top of the boundary layer instead of the measured aircraft winds at the specific *OF* altitudes. This will now be further discussed for the two flight days.

5. October 5, 2021 Mass Balance Flight Results

The winds for the October 5, 2021 flight were highly favorable for a mass balance analysis. The winds on this day ranged between 7.3 and 8.2 m/s for the flight legs further studied. **Initially, only two *OF* flight legs were identified, but our re-analysis identified part of an additional *OF* leg that could be employed.** Figure 6 shows the flight tracks with the CH_4 measurements superimposed by circular points. In this and all subsequent plots the circular points are colored and sized by the measured concentrations.

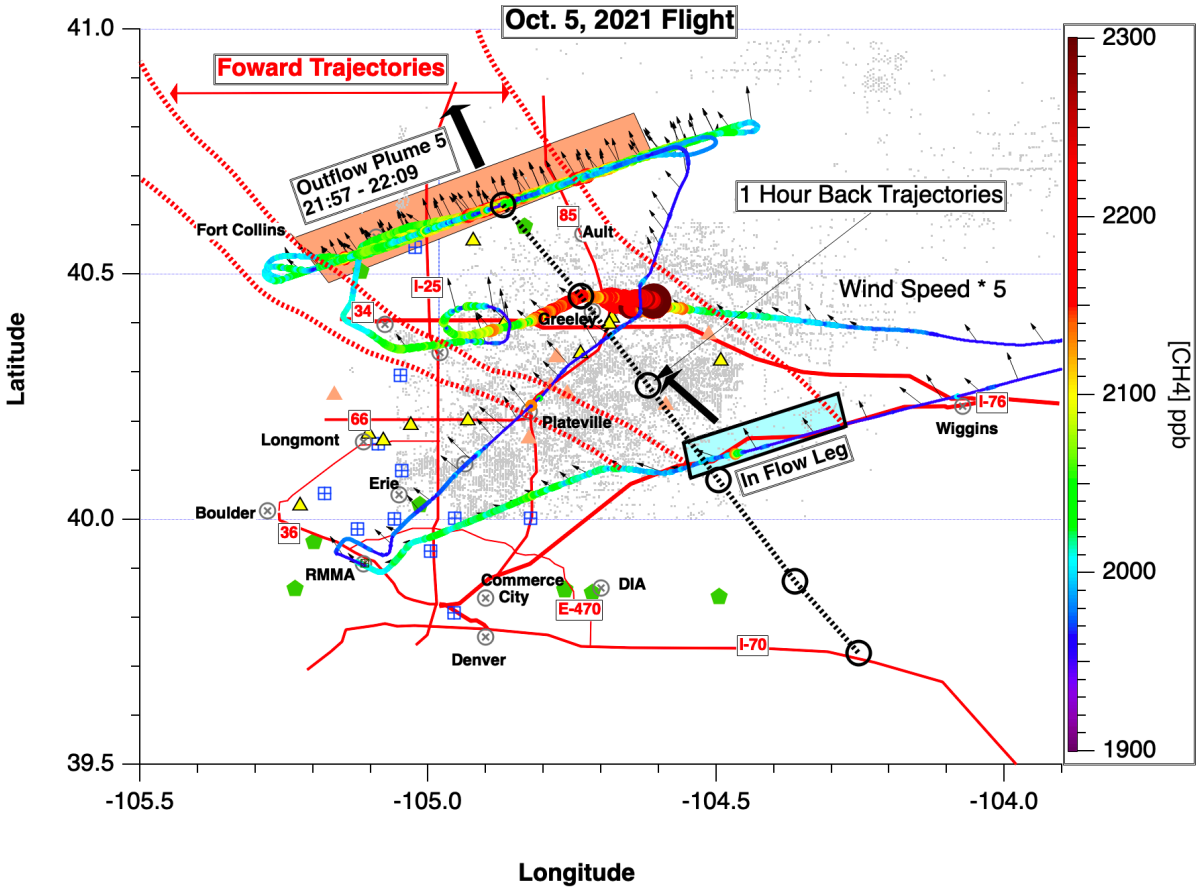

Figure 6: Oct. 5 flight tracks colored by the measured CH_4 concentrations. Each of the measurement points are further sized by the CH_4 concentrations. Plume *OF* leg 5 is highlighted by the orange colored box, which represents the approximate coordinates for two other *OF* legs acquired at different altitudes downwind of the *IF* leg indicated by the blue colored box. The red and black dashed lines show the forward and back trajectories, respectively. For clarity many of the emission source symbols shown in previous figures have been eliminated here.

We show in this plot the *IF* time period and one of the *OF* leg time periods (Plume 5). These time periods have been identified using time series concentration plots, which were then further supported with the help of forward (dark dashed red lines) and back trajectories (dark dashed black lines with open circles) in 1-hour increments. The *IF* forward trajectories intersect the plume *OF* regions, and importantly, these forward trajectories reveal that large upstream contributions from Commerce City (Suncor Refinery)/Denver VOC sources did not contribute to the *IF* leg. In fact,

the forward trajectory slightly to the west of the *IF* box veers further to the northwest and is not part of the *OF* sampled region. The mid plume *OF* back trajectory traces back to the *IF* region and indicates a basin transit time of approximately 3 hours. The large black arrows designate the average Plume 5 *OF* and *IF* wind directions, as measured from the aircraft.

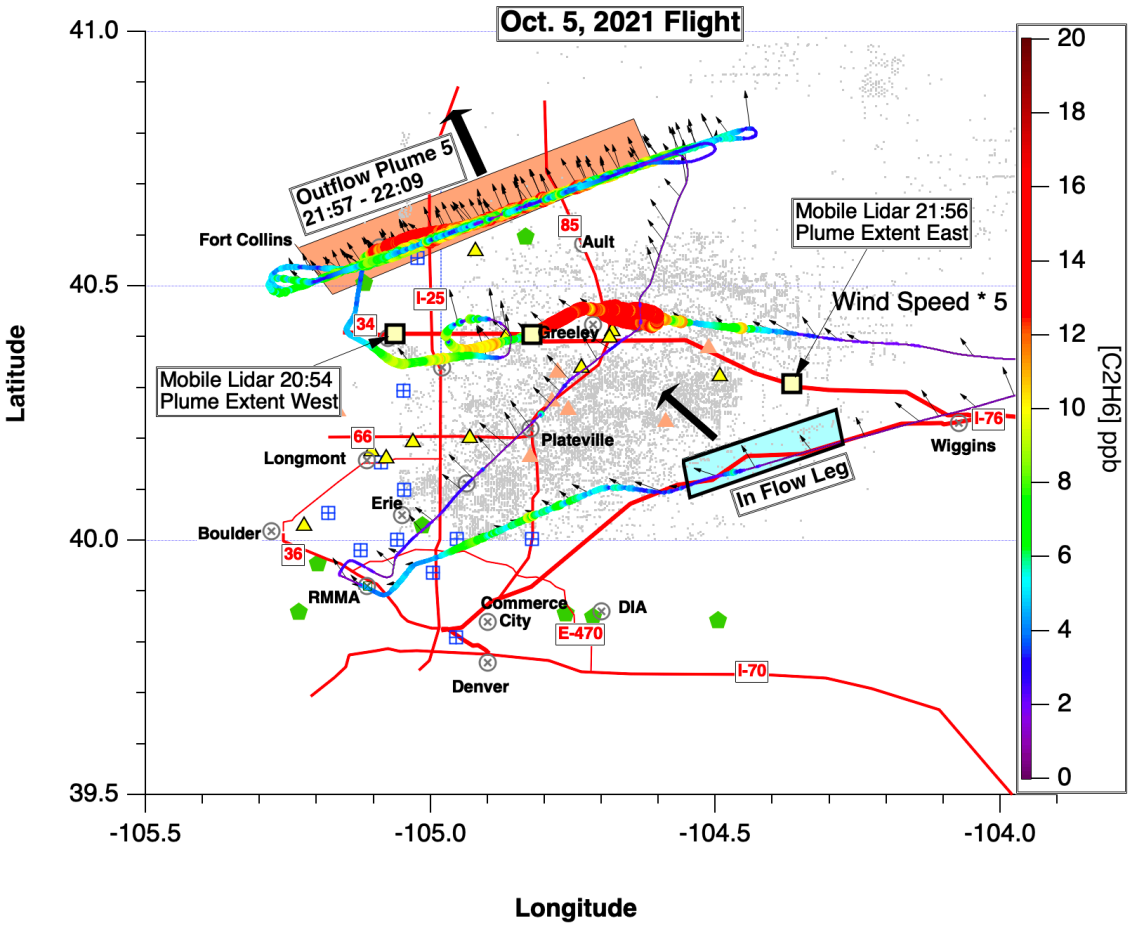

Figure 7: Oct. 5 flight tracks colored by the measured C_2H_6 concentrations. Each of the measurement points are further sized by the C_2H_6 concentrations.s

Figure 7 depicts the same plot as Fig. 6 only colored and sized by the measured C_2H_6 concentrations from the aircraft. This plot also shows the NOAA Mobile Lidar transit along route 34 from Loveland on the west side down to Wiggins on the southeast. This lidar van then returned to Loveland along this same path, both times passing through Greeley. As can be seen in the Oct. 5 and Oct. 1 flight tracks, the area around Greeley shows a persistence in significant CH_4 and C_2H_6 enhancements over background levels due to the high density of O&NG wells and processing facilities along with a high density of CAFOs activities. Hence the Mobile Lidar van passed through the heart of our DJB emissions influence domain. Despite a latitude offset with our aircraft *OF* legs, the vertically integrated lidar winds (wind speed and direction) along route 34 between the western and eastern lidar travel extents of Fig. 7 represents a reasonable surrogate for the overall basin winds. The resultant lidar winds from the surface to the top of the PBL along this track was determined by transforming the winds into u and v components, averaging and then

transforming back into the averaged wind speed and direction along this track. These values were then compared to the average aircraft winds measured over the basin at specific altitudes to derive correction factors that account for the full vertical wind extent. **The derived wind speed correction factor of 0.853 (lidar wind/aircraft wind) was applied to the wind speeds in the emission rate equation above. There was no wind direction correction as the ratio was 1.00. This same approach was applied to the data acquired on Oct. 1, and resulted in a wind speed correction of 0.891. The vertically integrated ML wind speed and direction standard deviations along the lidar end points were also employed in our error analysis. These represent conservative upper limits to uncertainties in the emission rates resulting from ambient variability. We acknowledge these are most likely overestimates in this error source.**

The final correction that was applied to the interim results is a correction to the MLH. As shown by the altitude profiles for the various constituents acquired during the in-progress vertical ascent from Greeley to Loveland (Fig. 8), the correct MLH for the Oct. 5 data should have been 1210 ± 100 m instead of our initial value of 1100 m. This linearly increased our final results for Oct. 5 by the ratio 1210/1100 = 1.10.

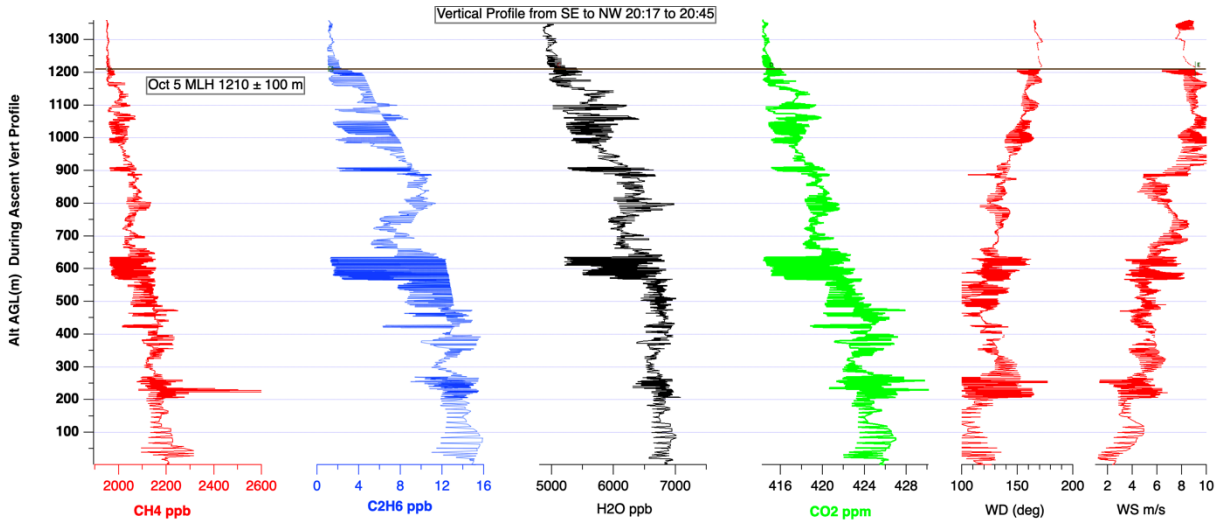

Figure 8: Vertical profiles for Oct. 5

This final report also includes an error analysis in our emission rate results based upon our best estimates for the uncertainties in each of the 7 variables (V_i) employed (MLH, ΔC, WS, WD, GS, T, P). This was accomplished by calculating the change of the emission rate with respect to each of the variables (∂ ER/∂V_i). These values were then used in the following quadrature addition sum to arrive at an estimated total 1σ systematic uncertainty (ΔER_j) in the emission rate for each *OF* leg intercept, *j*:

$$\Delta ER_j = \{ \Sigma \ [(\partial \, ER/\partial V_i) \, \sigma_i]^2 \}^{1/2}$$

The σ_i values in this expression were in turn estimated from the quadrature addition of the various term uncertainties, which in all cases was dominated by the conservative upper limit in the WS standard deviations. Table 3 lists the Oct. 5 CH_4 and C_2H_6 ER results in metric tonnes/hour (10^6 grams/hour) for each of the 3 *OF* legs in our final analysis along with the resulting 1σ estimated uncertainties.

Table 3: The ERs using $[CH_4]_{bkg}$ = 1969.7 ppb and $[C_2H_6]_{bkg}$ = 1.867 ppb and MLH = 1210 m. The Aircraft altitudes are the leg averaged values above ground level.

OF Leg	Times	Aircraft Altitude m	ER CH_4	ER C_2H_6
3	21:30:38 – 21:38:10	753	29.5 ± 7.5	4.2 ± 1.1
4	21:46:46 – 21:53:17	917	33.5 ± 11.1	4.6 ± 1.6
5	21:57:36 – 22:09:07	1084	26.5 ± 7.8	3.2 ± 1.2

The final major update to our interim report involves attempts at estimating the percentage of the measured CH_4 emission arising from O&NG and from CAFOs activities based on a number of approaches. We initially estimated this from the correlation coefficients of methane-ethane linear regressions. This approach relies on the fact that methane and ethane are highly correlated from O&NG activities and not from CAFOS, and the r^2 correlation coefficient indicates the variance of methane that correlates with ethane, and hence the O&NG contribution. We re-visited this approach with a more thorough examination of the data employed in this analysis. This included: an orthogonal distance regression (ODR) analysis of the original 1-second data instead of the 11-point smoothed data; careful removal of duplicate data points sometimes reported by certain instruments; selection of data in the appropriate DJB influence domain (to be discussed and further shown in Fig. 10) which further reside in the PBL; and careful data inspection to insure that the CH_4 and C_2H_6 data are properly co-aligned in time. Datasets misaligned by as little as 1-second can yield erroneously low correlation coefficients.

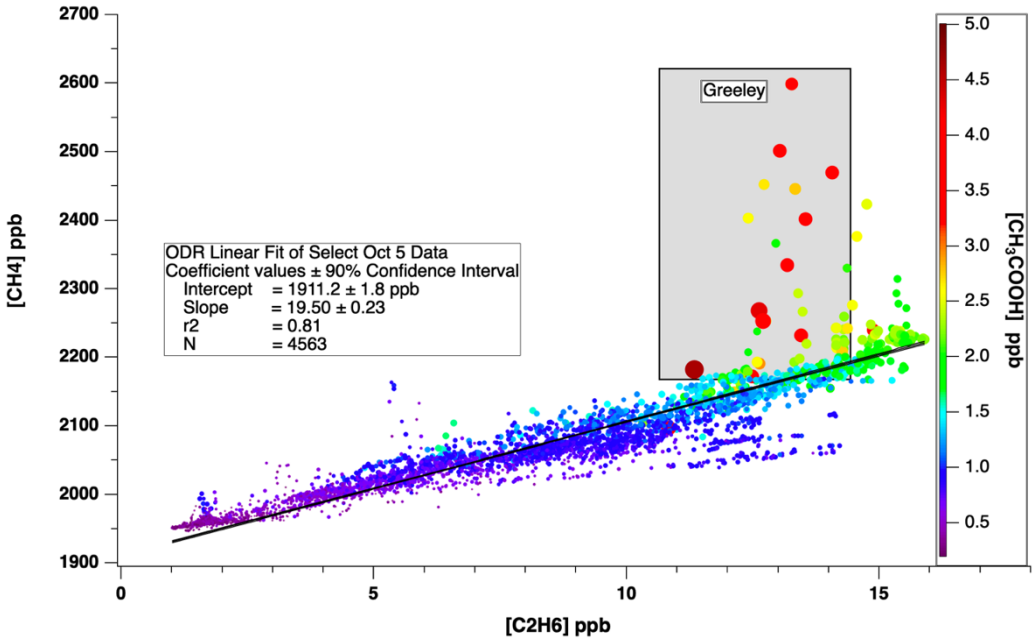

Figure 9: ODR linear regression with 90 % confidence intervals for the select Oct. 5 data. The data points are colored and sized by the measured acetic acid (CH_3COOH). The highlighted box shows data acquired around Greeley, CO.

Figure 9 provides an example of this approach. The ODR linear fit was carried out over the select 4563 data points described above. This yields a regression correlation coefficient (r^2) of 0.81, which provides one estimate for the O&NG contribution for the select data of Oct. 5 residing in the PBL influence domain. The data of Fig. 9 are colored and sized by the measured acetic acid (CH_3COOH) concentrations acquired from the onboard PTR-TOF-MS instrument. The ground-based studies by Yuan et al. (2017) have identified acetic acid as one of many useful CAFOs

tracers. As indicated by that study, enhanced emissions of CH_3COOH emanate from the feedyard waste associated with chickens, sheep, and beef. Figure 9 indeed shows such CH_3COOH enhancements centered around the Greeley, CO area for the Oct. 5 flight where some of the largest CAFOs facilities are located. The data highlighted in the gray box shows enhanced CH_4 from the Greeley CAFOs with minimal C_2H_6 enhancements.

Utilizing CH_3COOH measurements in conjunction with our measurements of CH_4 and C_2H_6, we carried out additional analysis based upon a multivariate linear regression approach following the approach presented by Kille et al. (2019). In our analysis, we only considered data in the PBL DJB influence domain (to be discussed). In this approach, the measured enhanced CH_4 concentrations above a basin background, $\Delta[CH_4]_{measured}$, can be described by the linear sum of three terms: B_0, representing a CH_4 source term that is neither associated with O&NG nor CAFOs; a term associated with O&NG, as defined by the product $B_1 * \Delta[C_2H_6]$; and a term associated with CAFOs defined by the product $B_2 * \Delta[CH_3COOH]$.

$$\Delta[CH_4]_{measured} = B_0 + B_1 * \Delta[C_2H_6] + B_2 * \Delta[CH_3COOH]$$

In all cases, the same select dataset employed in the correlation coefficient analysis method was employed here. For the Oct. 5 flight, the basin background *IF* CH_4 and C_2H_6 concentrations of 1969.7 ppb and 1.867 ppb, respectively, were used:

$$\Delta[CH_4]_{measured} = [CH_4]_{measured} - 1969.7 \text{ ppb}$$

$$\Delta[C_2H_6]_{measured} = [C_2H_6]_{measured} - 1.867 \text{ ppb}$$

Determining the basin background $[CH_3COOH]$ was somewhat more challenging. The CH_3COOH CAFOs enhancements were typical only a few ppb, which makes the multivariant regression approach very sensitive to the background CH_3COOH values selected. Just as important, accurately determining the basin background CH_3COOH values required a careful selection of the data to avoid positive biasing the background values by including data around Greeley and data from the *OF* legs. On Oct. 5, this analysis yields:

$$\Delta[CH_3COOH]_{measured} = [CH_3COOH] - 0.450 \text{ ppb}$$

The multivariate linear regression yields the coefficients B_0, B_1 and B_2, which are then used in the following expressions to derive the percentage contributions from O&NG, CAFOs, and other CH_4 sources:

$$\% \text{ O\&NG} = \frac{\Sigma B_1 * \Delta[C_2H_6]}{\{\Sigma B_0 + B_1 * \Delta[C_2H_6] + B_2 * \Delta[CH_3COOH]\}}$$

$$\% \text{ CAFOs} = \frac{\Sigma B_2 * \Delta[CH_3COOH]}{\{\Sigma B_0 + B_1 * \Delta[C_2H_6] + B_2 * \Delta[CH_3COOH]\}}$$

$$\% \text{ Other} = \frac{\Sigma B_0}{\{\Sigma B_0 + B_1 * \Delta[C_2H_6] + B_2 * \Delta[CH_3COOH]\}}$$

We carried out this analysis employing two different regions of influence. The first involved the PBL dataset depicted by the large combined light and dark blue colored areas of Fig. 10. These bounds were selected by the *OF* back trajectories. The second area of influence is even more restrictive and is depicted by the lighter-colored trapezoid of Fig. 10. The bounds here were determined by the forward trajectories shown in Fig. 6, and this influence domain represents the data domain used in Fig. 9.

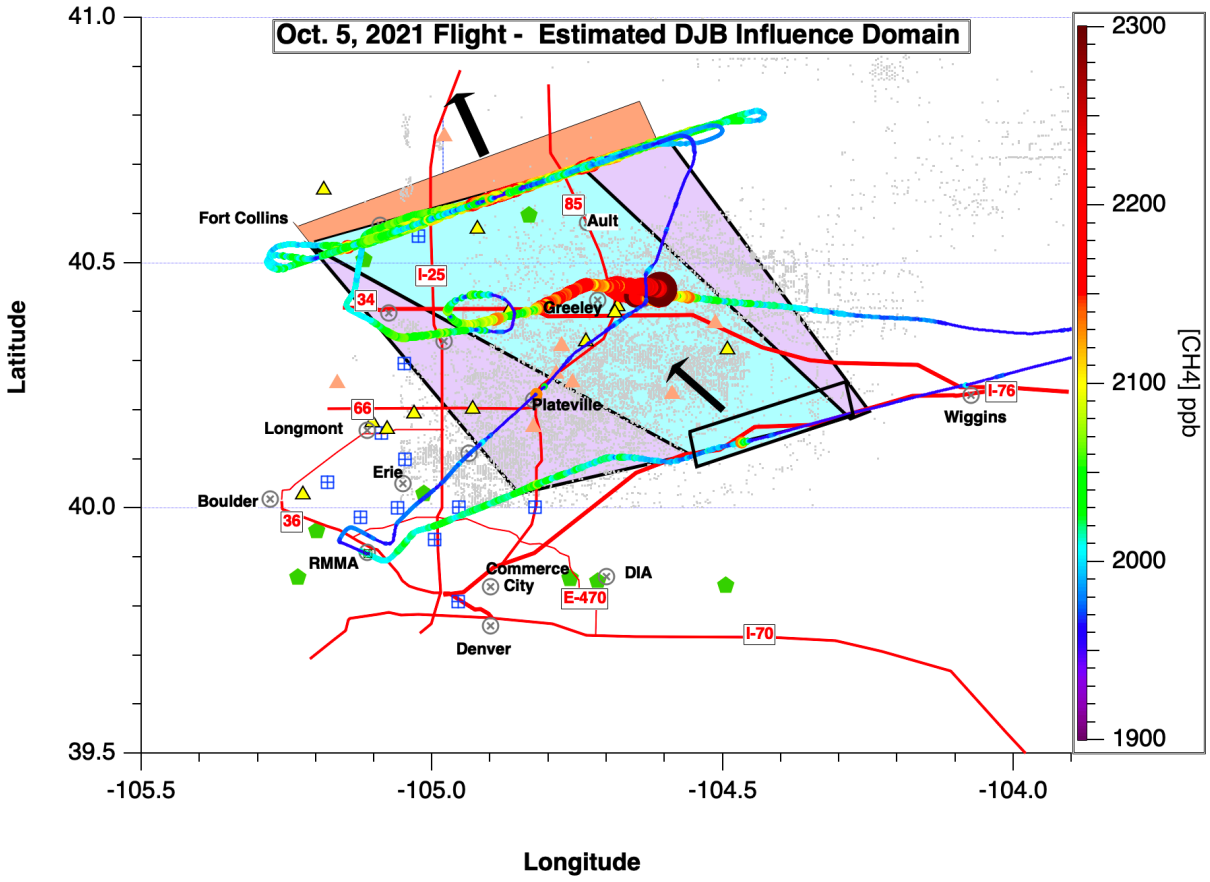

Figure 10: Oct. 5 DJB estimated regions of influence in the PBL defined by the *OF* back trajectories (large rectangle) and the *IF* forward trajectories of Fig. 6 (lighter blue trapezoid).

We note that the larger extent defined by the back trajectories, particularly on the west side, most likely include data not truly in our region of influence. This larger influence region includes additional sources of CH_4 from O&NG sources, as shown by Fig. 10 and the C_2H_6-colored flight tracks of Fig. 7. It is important to note that these back trajectories were calculated starting from the aircraft *OF* regions, which occurred ~ 2 hours after the *IF* and thus do not truly represent the airmass sweeping across the basin. Hence, we believe that the more restrictive influence region defined by the forward trajectories (light blue trapezoid) is a better representation of the basin influence region. However, as can be seen in Fig. 10, most of the large CH_4 sources are embedded in both boxes, centered around Greeley, and thus the source attribution results from the larger domain should only be marginally higher than the more restrictive domain. This is borne out by

the results for the 2 areas of influence shown in Table 4. In both cases the other sources of CH_4 from neither O&NG or CAFOs are near 0.

Table 4: Oct 5 source attribution estimates for 2 different PBL regions of influence

Region of Influence	O&NG % Contribution	CAFOs % Contribution
Larger Region from *OF* Back Trajectories	76%	24%
Smaller Region from *IF* Forward Trajectories	72%	28%

These results are close to the 81% O&NG contribution from the correlation analysis, and our **best estimate for the Oct. 5 O&NG contribution resides in the 72% to 81% range. A similar analysis for the Oct. 1 data yields an O&NG range of 58% to 72%, employing the multivariant approach and the correlation approach (see Fig. 12), respectively.** In the multivariant approach we used the following for our Oct. 1 background values: $[CH_4]_{background}$ =1981.6 ppb, $[C_2H_6]_{background}$ = 2.484 ppb, and $[CH_3COOH]_{background}$ = 0.535 ppb. The Oct. 1 multivariant contributions from CAFOs and other sources are, 23% and 19%, respectively. An average of all 4 determinations yields a mean O&NG contribution of 71% ± 10% for the two study days.

It is important to note that we are continuing to investigate the veracity of both source apportionment approaches for other flight days even after submittal of this final report. We are particularly interested in identifying regions where O&NG and CAFOs sources are further separated spatially than the present data. This will allow us to further test the discriminatory power of these approaches in separating these two sources. We are also investigating the use of other trace gases in this effort.

6. October 1, 2021 Mass Balance Flight Results

Figures 4a,b show the Oct. 1 flight tracks, colored and sized by measurements of CH_4 (Fig 4a) and C_2H_6 (Fig 4b) superimposed. Two valid *OF* legs have been identified, and Table 5 presents the results carrying out the same analysis procedures as Oct. 5. We note the larger systematic uncertainty estimates for this flight day, and these are due to the very light winds in the 2 to 3 m/s range and the associated larger wind speed variance determined from the mobile lidar measurements. In addition, the forward and back trajectories on this day did not yield the same consistent picture as those on Oct. 5. Figure 11 shows the vertical profile measurements employed in determining the PBL (MLH) on this day.

Table 5: Oct. 1 ERs in metric tonnes/hr using $[CH_4]_{bkg}$ = 1981.6 ± 2.9 ppb and $[C_2H_6]_{bkg}$ = 2.484 ± 0.125 ppb and MLH = 1317 m. The Aircraft altitudes are the leg averaged values above ground level, and the uncertainties are the 1σ systematic estimates.

OF Leg	Times	Aircraft Altitude m	ER CH_4	ER C_2H_6
1	21:19:30 – 21:56:28	287	17.1 ± 14.3	1.8 ± 1.4
5	22:02:35 – 22:10:20	595	19.9 ± 14.0	1.9 ± 1.4

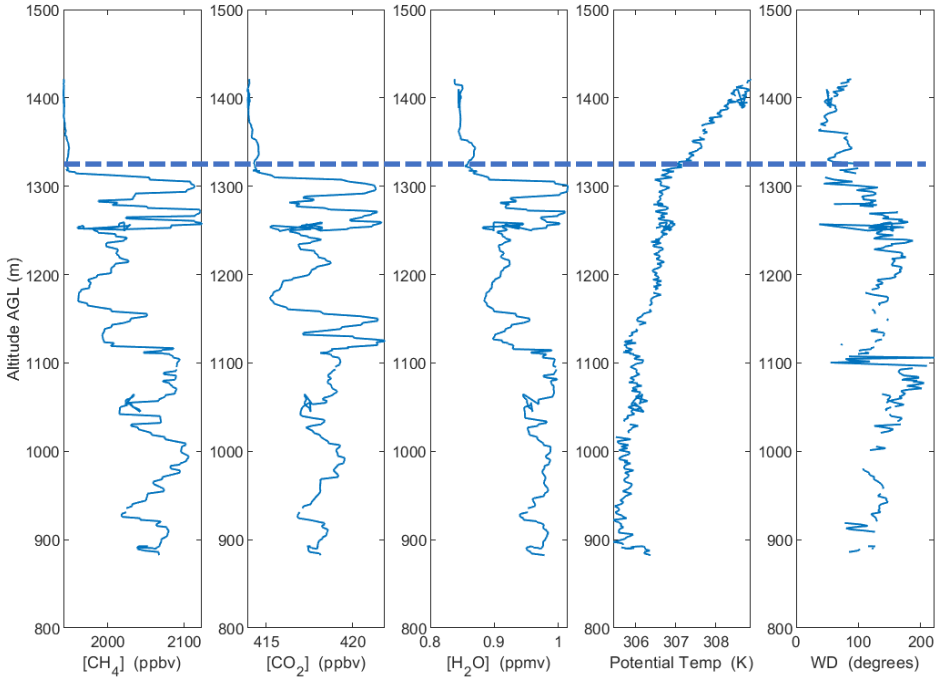

Figure 11: Vertical profiles acquired during the enroute flight ascend between Greeley and the western edge of the flight track near Longmont, CO. The dashed line indicates a mixed layer height (MLH) of 1317-m above ground level.

Similar to Fig. 10, we derived an effective DJB influence domain for the Oct. 1 flight, and this is shown in Fig. 12. This was based upon the forward and back trajectories, and the wind vectors. As can be seen, the two large landfill CH_4 sources are not included in this influence region.

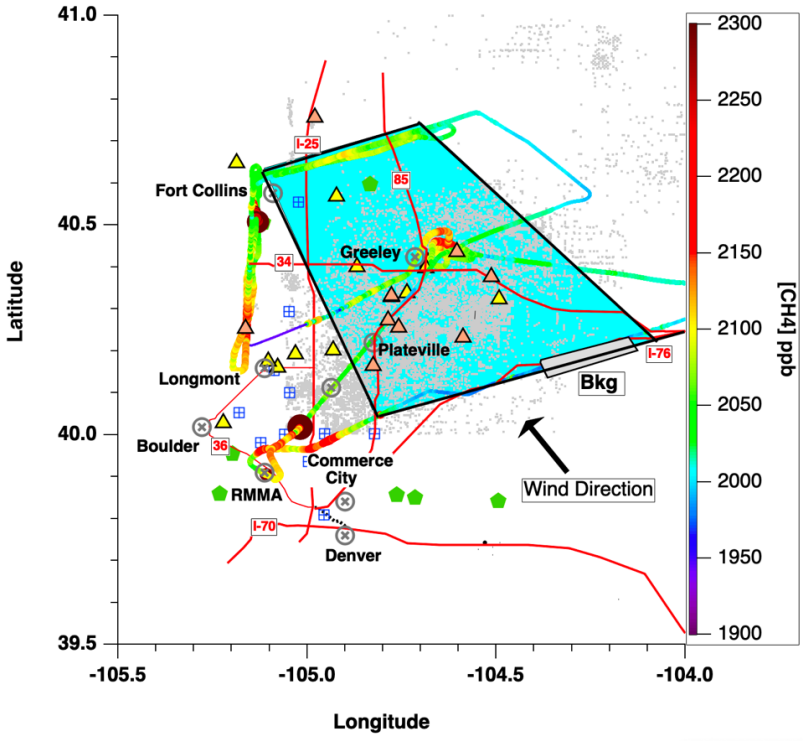

Figure 12: Oct 1 flight with the estimated influence domain, defined by the trajectories.

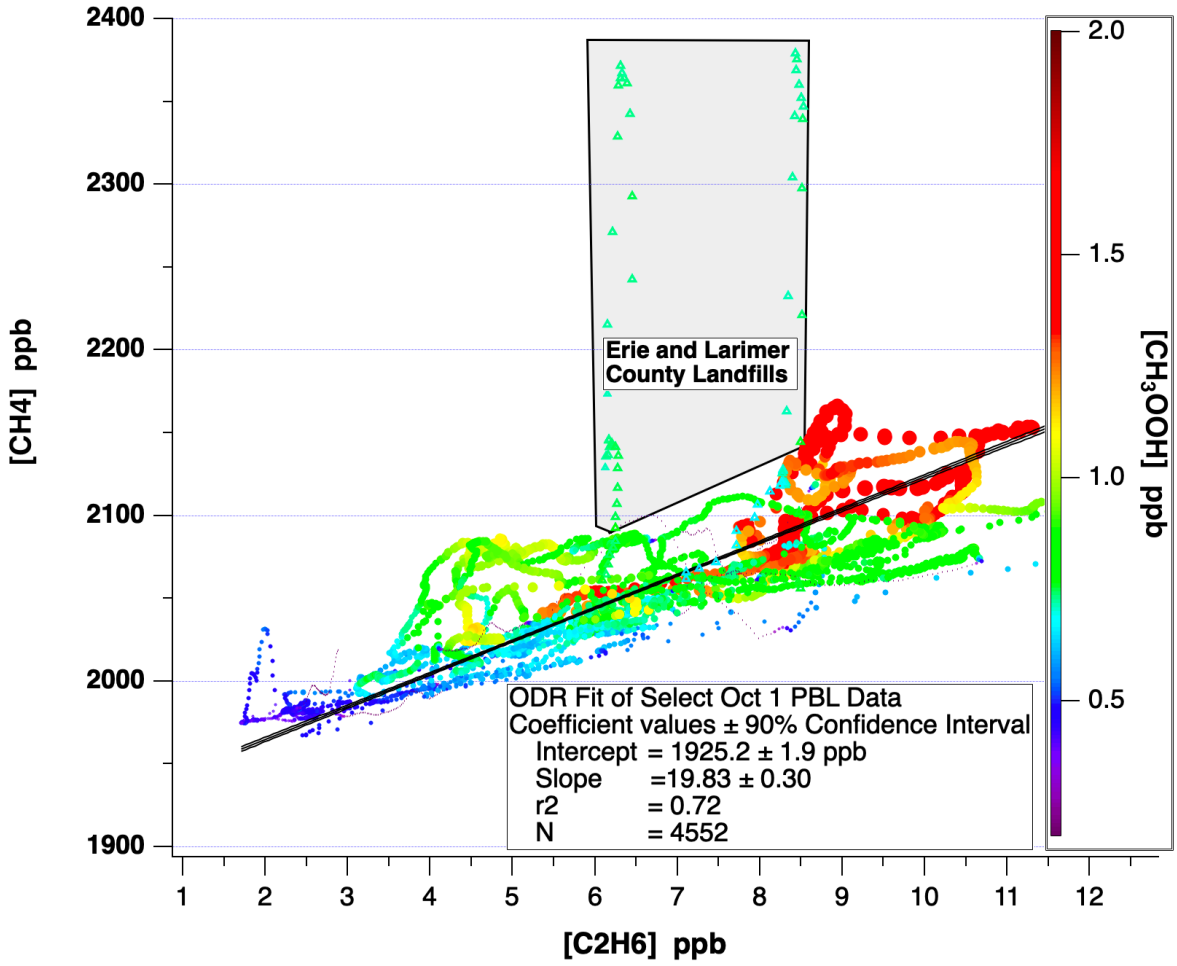

Figure 13: ODR linear regression results for data acquired in the select influence domain on Oct.1. The data are colored and sized by the CH_3COOH measurements.

Figure 13 shows the resultant Oct. 1 linear ODR regression for the select data in the influence domain of Fig. 12. The nearly equivalent slope as Oct. 5 suggests that the overall basin emission ratios have not changed between these two days. The correlation coefficient on this day was 0.72, which we estimate as the upper bounds for the O&NG contribution. Due to the low wind speeds our measurements over the two large landfill sites (Erie and Larimer County near Fort Collins) show significantly enhanced CH_4 with no C_2H_6 enhancements. These data are highlighted in the light gray box and are colored and sized by CH_3COOH. As can be seen, the CH_3COOH concentrations, which range between 0.710 to 0.765 ppb, are not enhanced over the two landfills. This result was somewhat surprising. However, it indicates that enhanced landfill sources of CH_3COOH can be ruled out as one of the potential additional CH_3COOH sources that could confound our multivariant regression analysis, at least for the temperature conditions found on these two days. Also shown in Fig. 12 is the CH_3COOH contribution to CH_4 from CAFOs. Like the Oct. 5 data, these data show the largest positive deviations from the fit line. Our interim report includes many more additional details for the Oct. 1 mass balance results, but for the sake of brevity are not included here.

7. Summary of October 1 and October 5 Mass Balance Flight Results & Comparisons with Previous DJB Studies

Table 6: Summary of CH_4 and C_2H_6 Emission Rates (ER) in 10^6 grams/hour (metric tonnes/hr) along with 1σ systematic uncertainty estimates.

Flight Date	*OF* Leg	ER CH_4	Uncertainty (1σ)	ER C_2H_6	Uncertainty (1σ)
Oct. 1	1	17.1	14.3	1.8	1.4
Oct. 1	5	19.9	14.0	1.9	1.4
Oct. 5	Portion 3	29.5	7.5	4.2	1.1
Oct. 5	4	33.5	11.1	4.6	1.6
Oct. 5	5	26.5	7.8	3.2	1.2
Overall Avg		**25.3 ± 8.4**		**3.1 ± 1.4**	

The last row shows the net overall average emission rates with the total combined uncertainties at the 1σ level. This was obtained from the quadrature addition of the standard deviation of the mean for the five measurements (6.8 MT/hr for CH_4 and 1.3 MT/hr for C_2H_6) with the average systematic uncertainties (5.1 for CH_4 and 0.6 for C_2H_6). The latter was obtained from the quadrature addition of the five systematic uncertainty terms divided by 5, which assumes that the individual systematic estimates are independent. Based upon our two analysis approaches, we derive an estimated O&NG contribution in the range of 58% to 81% for these two flight days, the average of which (4 determinations) yields a mean O&NG contribution of 71% ± 10%.

Our final results are higher than our interim results by 9% for CH_4 and by 48% for C_2H_6, but are within the mutual uncertainty estimates of one another. Table 7 is a repeat of Table 2 found in the Executive Summary Section of this report. This table shows the excellent agreement of our final CH_4 emission rates with other studies, particularly the University of Arizona study, which was carried out over the same time period and over approximately the same domain. It is also worth noting that the total DJB CH_4 emission rates have not changed over 9 years, despite a factor of ~ 2 increase in natural gas production over the DJB from 2015 to 2021. Also, our source attribution estimates from O&NG are within the ballpark of all previous studies.

Table 7: Final Results Based Upon Our Reanalysis in this Report & Comparisons with Other DJB Studies

Study Period	Total CH_4 ER	O&NG CH_4 % Estimates	Total C_2H_6 ER
Petron May 2012	26.0 ± 6.8	74 ± 33%	
Peischl April 2015	24 ± 5	75% ± 37%	7.0 ± 1.1
Kille March 2015		63% ± 17%	
Univ. of Arizona Sept/Oct 2021	25 ± 7	79%	
This Study Oct. 2021	**25.3 ± 8.4**	**71% ± 10%**	**3.1 ± 1.4**

Despite the CH_4 agreement, the C_2H_6 emission rate has decreased by a factor of 2.3 since the 2015 Peischl study. The reasons for this are still unclear. This could imply that the 2015 Peischl study may have been preferentially sampling enhanced C_2H_6 emissions from leaking storage tanks

where the CH_4 has been largely removed at the well head. Another possibility being investigated by the PIs of this report and by Professor Daniel Zimmerle at CSU relates to improved well-head technologies involving the addition of a 3rd stage of pressure reduction that has been implemented in recent years. This additional pressure reduction could reduce the amount of C_2H_6 emitted from tank venting. The precise year(s) when these improvements have been implemented and the percentage of wells employing these improvements is yet to be determined. However, these improvements most likely were not in place during the 2015 Peischl study.

Fortunately, there were additional measurements of C_2H_6, CH_4 and other gases carried out in the PBL over the DJB in 2014, and a comparison of Box-and-Whisker distributions with those from our 2021 study provide hints of changing C_2H_6 emissions. Figure 13 and the tabulations in Table 8 show C_2H_6 measurements acquired by the CU group using a similar C_2H_6 spectrometer on NCAR's C-130 during the 2014 FRAPPÉ study and C_2H_6 measurements from the Aerodyne group on NASA's WP3 aircraft during this same 2014 time frame during the DISCOVER-AQ study.

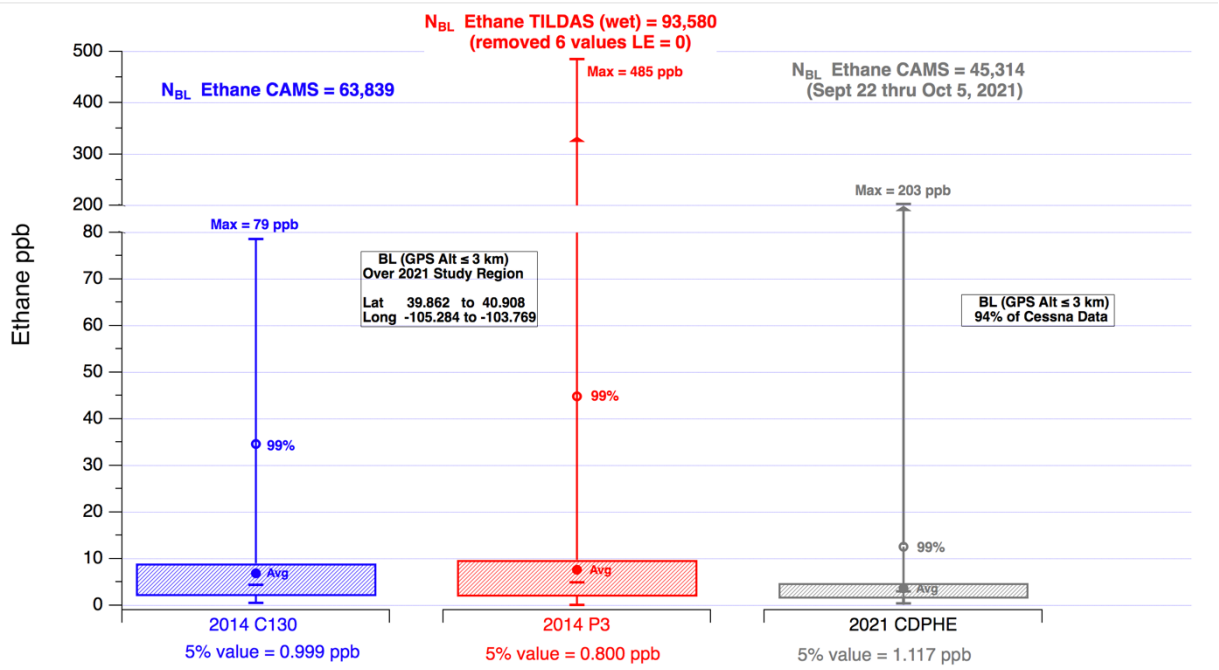

Figure 13: Comparison of C_2H_6 distributions in the boundary layer over the DJB. The boxes represent the 25 and 75% values while the medians are indicated by the horizontal lines in these boxes. In all cases, only data within an assumed boundary layer (BL) of 3 km (altitude above mean sea level) were compared.

Table 8: Comparison of C_2H_6 measurements employing similar IR spectrometers in the boundary layer over the DJB. The 2014 C130 and 2021 Cessna measurements employed similar CU IR spectrometers, calibration, and zeroing methods. The 2014 WP-3 measurements were carried out by Aerodyne Inc.

Measurement	Avg ± Std ppb	Median
2014 C-130	6.801 ± 7.098	4.356
2014 WP-3	7.629 ± 9.713	4.870
2021 Cessna	3.888 ± 3.152	3.202

The median boundary layer C_2H_6 values in 2014 relative to 2021 are 36% to 52% higher, and the average values are nearly a factor of 2 higher. With the exception of the one very large enhanced C_2H_6 concentrations measured near Greeley airport during 2021, where C_2H_6 values reached 203 ppb, the 99 percentile 2014 C_2H_6 data ranged between a factor of ~ 3 to 4 times higher than those in 2021. These 2021-2014 comparisons thus support the suggestion that earlier studies may have sampled more C_2H_6 emissions from various well pad leak sources, including storage tank emissions. Because of the importance of this finding, particularly as it relates to a potential ozone production from C_2H_6 oxidation by OH, this is clearly an area requiring further study.

8. Additional Analysis Employing Transport Models

Background: To provide an independent means of evaluating methane emissions form the Denver-Julesburg Basin, we have developed a WRF-CMAQ modeling system with the addition of GHG's (CH_4 and CO_2) as inert-tracers – proof of principle is presented here. Nested WRF domains with spatial resolution of 12, 4, and 1.33 km were created to provide high-resolution meteorological fields for CMAQ (Fig 14). This model predicts concentrations of trace gases inert on time scales of days as well as reactive gases such as ozone [*Canty et al.*, 2015; *He et al.*, 2020; *Hembeck et al.*, 2022]. For short-lived air pollutants, we used the U.S. EPA National Emissions Inventory (NEI) data, while EGDAR v6.0 GHG global emissions inventory [*Pagani et al.*, 2022; *Solazzo et al.*, 2021] and NOAA Carbon Tracker datasets were selected to provide GHG emissions in CMAQ. This modeling tool can provide 3-dimensional information, such as emissions, transport, and conversions, of GHG in a consistent modeling system, especially useful for quantification of pollutant fluxes and the emissions inventory.

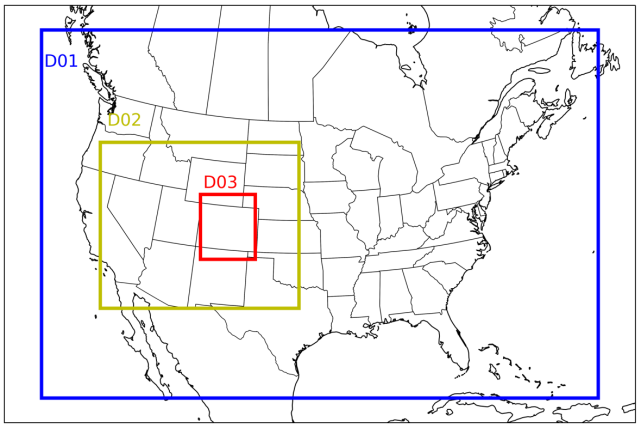

Figure 14: WRF domains proposed for the Colorado GHG study. D1, D2, and D3 stand for 12, 4, and 1.33 km, respectively.

The objective of this effort is to set up and test the model to demonstrate that it compiles, runs, and generates physically meaningful concentrations for the domain over Colorado. When the new contract is in place, we will verify that the meteorological variables from WRF track observations, adjust or nudge as necessary, then test new emissions inventories provided by CDPHE. The WRF simulations were driven by the NCEP FNL reanalysis data. We conducted observation and analysis nudging to improve the simulations of meteorological fields following the method developed for

the DISCOVER-AQ campaign. CMAQ was run for 09/01/2021 to 10/07/2021. A summary of accomplishments thus far includes:

- Added CO_2 and CH_4 into the CMAQ model as inert tracer.
- For Sep. and Oct. 2016, added global background 412.38/413.83 ppmv CO_2 and 1.9026/1.9080 ppmv into the IC and BC.
- Re-gridded the EDGARv6.0 GHG emissions (0.1° resolution) into CMAQ 12/4/1.33 km domains.
- Re-gridded Carbon Tractor biogenic GHG flux (1.0° resolution) into CMAQ 12/4/1.33 km domains.
- CMAQ simulations from 09/01/2021 to 10/07/2021 with the first two weeks as spin-up. Decompose GHG conc. into background (from ICBC) and enhancements (from emissions).
- Begun comparing CMAQ results with Cessna flight observations (Sep. 17, 22, 23, 24, 27, 28, Oct. 1, 5).

Initial results indicate that WRF does a good job with temperature and pressure but underestimates absolute humidity by about 20% (Figure 15). We will compare the modeled winds to measurements next. The modeled methane and carbon monoxide are reasonable for a first run (Figure 16) with simulated plumes located near where they were observed. Comparison of methane to aircraft observations suggests that EDGAR v6.0 underestimates local emissions and that the background used may be a bit low. The correlation coefficient, r, is 0.69 and the slope in the model vs. measurements is 0.74 with a mean difference (negative bias) of ~39 ppb out of about 2000 ppb. Similar results are seen for CO but the higher r-value (0.84) points to boundary conditions with underestimated CO.

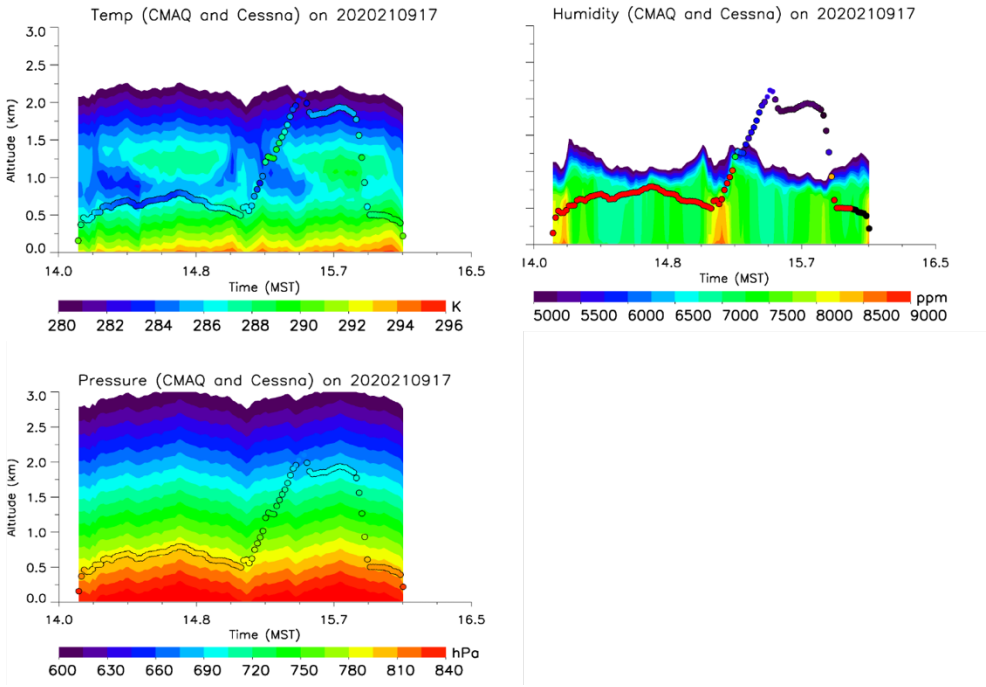

Figure 15: CMAQ results (background) and Cessna observations (circles) for 17 September 2021. The background (curtain) shows CMAQ output for the times and altitudes of the aircraft locations. The colored circles indicate observations from the Cessna.

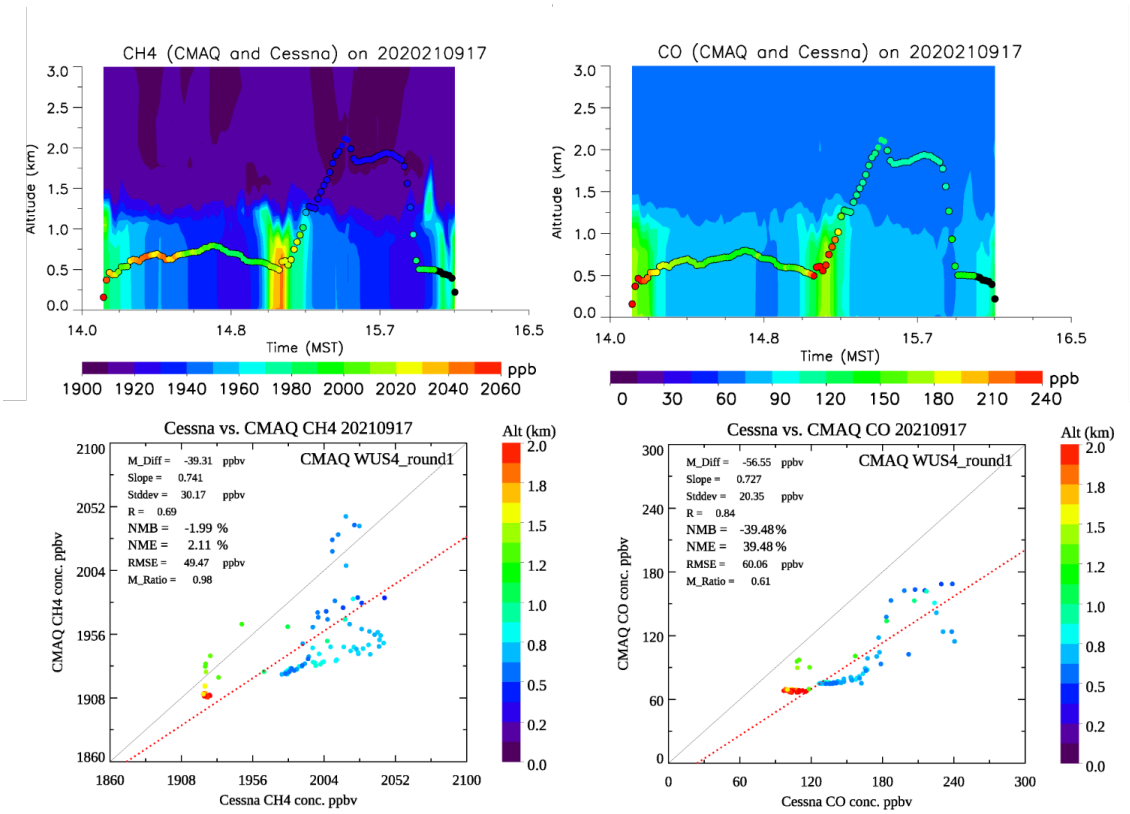

Figure 16: Same as Figure 15, but for trace gas concentrations. CMAQ is generally underestimating CH_4 and CO but correlates reasonably well.

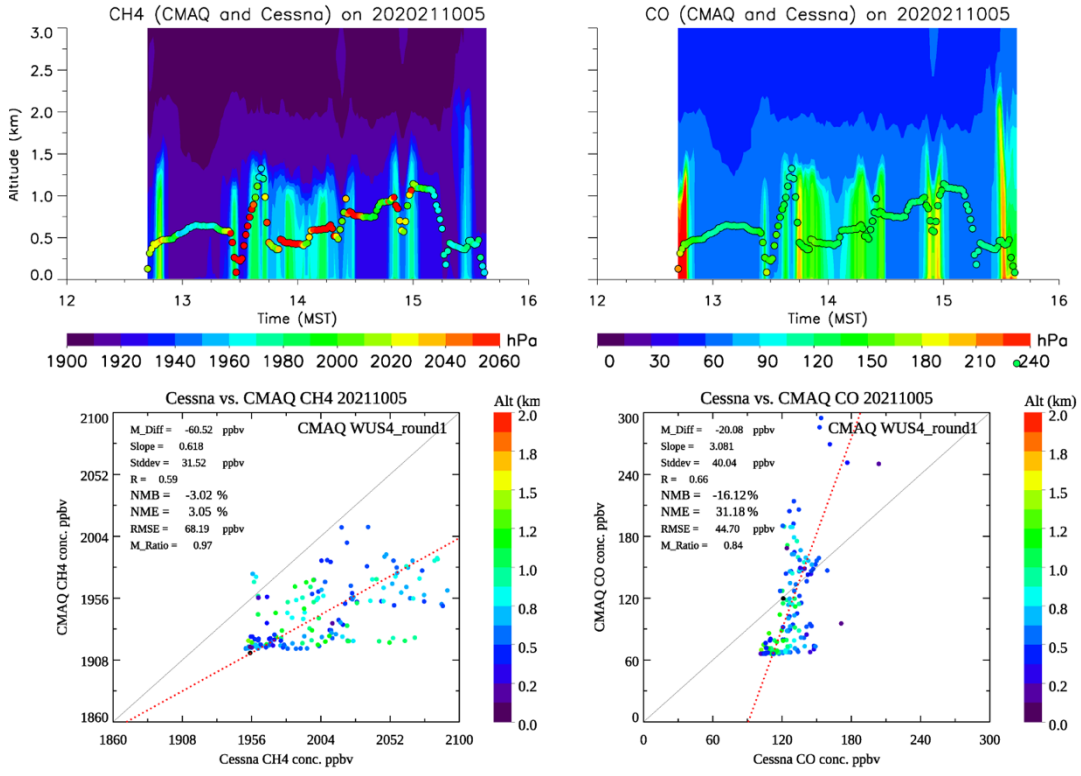

Figure 17: Same as Figure 16 but for 5 October 2021. Emissions of methane may be higher than in EDGAR6.0 while emissions of CO might be lower on this day.

The results for 5 October 2021 are similar (Figure 17) to September 17. Locations of plumes are approximately correct but the magnitude for CH_4 is too low; both the slope and average values are low. For methane the answer may be stronger local emissions. For CO on this day the average modeled concentration is too low but the slope is high suggesting that emissions may be too high. CO however is sensitive to local traffic and a challenge for a global model that cannot represent small scale fluctuations in road travel.

8.1 Summary and Next Steps.

Initial investigations prove that CMAQ can be used to simulate methane and other trace gases over Colorado. Results can be compared directly to aircraft (or other) observations and there is no sign of substantive errors in the code. The preliminary work is finished. The entire period of the 2021 field campaign has been run, and comparisons to other flight days will be performed. It is straightforward to rerun CMAQ with a different set of gridded emissions or with a multiplier on the EDGAR v6.0 data.

It is not yet possible to evaluate methane emission rates from CAMQ runs. Differences between model and measurements can result from small errors in the meteorology or the emissions or both. Next steps will involve evaluating the WRF winds against Cessna and lidar measurements. WRF can be nudged with observations to better represent the state of the local atmosphere at the time of the flights. When the meteorology in WRF best represents the observed weather, we will adjust the emissions. First by substituting a local, high-resolution emissions model selected by CDPHE for the 2021 inventory. This should produce better results than a national (EPA) or global model such as EDGAR. If this produces good agreement with spatial and temporal trends, we will adjust the absolute magnitude of emission rates to best match observations. If EDGAR v6.0 or the EPA inventory produce better correlations with observations we will adjust these models. The optimized inventory can be perturbed to test for uncertainty in the method of evaluating emissions based on measurement-model comparisons. Not all flight days will have meteorology appropriate to make emissions inferences, but with this tool we expect to expand the number of usable days and add an independent means of evaluating methane emissions form oil and gas operations in the DJ Basin.

9. Major Summary Points of Present Study

- **Our best estimate of DJB methane emissions in 2021 is 25.3 ± 8.4 metric tonnes/hr with 71% ± 10 % from O&G operations.**
- **This agrees with results published by Cusworth et al. (2022), carried out over the same time frame and domain as this study, and with previous 2012 and 2015 studies**
- **Although production doubled since 2015, methane emissions in 2021 were the same within experimental uncertainty.**
- **Ethane emissions in contrast have fallen from ~7.0 to 3.1 metric tonnes/hr.**

10. Presentations & Planned Publications

Presentations

Daley, H et al. (2023, January 8-12) Aircraft-Based Mass Balance Approach to Determine Methane Fluxes in the Colorado, DJ Basin. 103 Annual Meeting American Meteorological Society, Denver, CO,

https://ams.confex.com/ams/103ANNUAL/meetingapp.cgi/Paper/420648

Publications Planned

Daley, H. M., A. Fried, P. Weibring, D. Richter, J. Walega, R. R. Dickerson, X. Ren, P. Stratton, A. Brewer, S. Baidar A. Koss, and J. Kimmel (2022), Methane, Ethane, & VOC Fluxes in the Colorado Denver Jules Basin, Fall 2021, Atmos. Chem. and Phys., in preparation.

A potential second publication may be submitted by Fried et al. regarding the significantly lower DJB ethane results compared to earlier studies, potential causes, and the implications on front range ozone levels. An additional publication(s) by He et al. will also be prepared discussing transport modeling results, comparisons with measurements, and upgrades to existing emission inventories.

References

Canty, T. P., et al., Ozone and NOx chemistry in the eastern US: evaluation of CMAQ/CB05 with satellite (OMI) data, *Atmospheric Chemistry and Physics*, ***15*****(19)**, 10965-10982, 2015.

Cusworth, D.H., et al., Strong methane point sources contribute a disproportionate fraction of total emissions across multiple basins in the United States, *Proceedings of the National Academy of Science,* **119 (38),** doi:10.1073/pnas, 2022.

He, H., et al., The long-term trend and production sensitivity change in the US ozone pollution from observations and model simulations, *Atmospheric Chemistry and Physics*, *20*(5), 3191-3208*,* 2020.

Hembeck, L., et al. Investigation of the Community Multiscale air quality (CMAQ) model representation of the Climate Penalty Factor (CPF), *Atmospheric Environment*, *283,* 2022.

Kille, N., et al., Separation of Methane Emissions From Agricultural and Natural Gas Sources in the Colorado Front Range, *Geophys. Res. Lett.,* **46,** 3990 - 3998, 2019.

Pagani, F., et al. EDGAR v6.1 Global Air Pollutant Emissions, *JRC Data Catalogue,* 2022.

Peischl, J., et al., (2018), Quantifying Methane and Ethane Emissions to the Atmosphere From Central and Western U.S. Oil and Natural Gas Production Regions, *J. Geophysics. Res.,* **123,** 7725 – 7740, doi: 10.1029/2018JD028622.

Pétrone, G. et al. (2014), A new look at methane and nonmethane hydrocarbon emissions from oil and natural gas operations in the Colorado Denver-Julesburg Basin, *J. Geophysics. Res.,* **119,** 6836 - 6852, doi:10.1002/ 2013JD021272.

Solazzo, E., et al. Uncertainties in the Emissions Database for Global Atmospheric Research (EDGAR) emission inventory of greenhouse gases, *Atmospheric Chemistry and Physics*, *21*(7), 5655-5683, 2021.

Weibring, P., D. Richter, J.G. Walega, A. Fried, J. DiGangi, H. Halliday, Y. Choi, B. Baier, C. Sweeney, B. Miller, K.J. Davis, Z. Barkley, and M.D. Obland, *Atmos. Meas. Tech*., **13,** 6095 – 6112, 2020.

Yuan, B., et al., Emissions of volatile organic compounds (VOCs) from concentrated animal feeding operations (CAFOs): chemical composition and separation of sources, *Atmos. Chem. Phys., **17,*** 4945 – 4956, 2017.